Refining geomagnetic field intensity changes in Europe between 200 CE and 1600 CE. New data from the Mediterranean region.

M. Rivero-Montero[1], M. Gómez-Paccard[1], F.J. Pavón-Carrasco[2], M.A. Cau-Ontiveros[3,4], L. Fantuzzi[4,5], F. Martín-Hernández[1,2], A. Palencia-Ortas[1,2], E. Aidona[6], E. Tema[7], D. Kondopoulou[6], C. Mas-Florit[4], J. Ramon-Torres[8]

[1]Instituto de Geociencias (IGEO) CSIC, UCM, c/Doctor Severo Ochoa, 7. Facultad de Medicina (edificio entrepabellones 7-8), Ciudad Universitaria, 28040-Madrid, Spain. E-mail addresses: m.rivero@csic.es; mgomezpaccard@csic.es.

[2]Dpto. de Física de la Tierra, Astronomía y Astrofísica I, Universidad Complutense de Madrid (UCM), Avd. Complutense s/n, 28040-Madrid, Spain. E-mail addresses: fjpavon@ucm.es; fatima@ucm.es; ali@ucm.es.

[3]ICREA, Pg. Lluís Companys 23, 08010 Barcelona, Spain.

[4]Equip de Recerca Arqueològica i Arqueomètrica de la Universitat de Barcelona (ERAAUB), Institut d'Arqueologia de la Universitat de Barcelona (IAUB); Departament d'Història i Arqueologia, Facultat de Geografia i Història, Universitat de Barcelona (UB), c/Montalegre, 6, 08001, Barcelona, Spain. E-mail: macau@ub.edu, cmas@ub.

[5]Universidad de Cádiz, Spain. E-mail: leandro.fantuzzi@uca.es.

[6]Aristotle University of Thessaloniki, Department of Geophysics, School of Geology, 54124 Thessaloniki, Greece. E-mail: despi@geo.auth.gr; aidona@geo.auth.gr.

[7]Università degli Studi di Torino, Dipartimento di Scienze della Terra, Via Valperga Caluso 35, 10125 Torino, Italy. E-mail: evdokia.tema@unito.it.

[8]Consell Insular d'Eivissa. E-mail: joanramontorres@gmail.com.

Abstract

Absolute past geomagnetic intensity values can only be recovered by investigating baked archeological and volcanic materials. Here we present 10 new archeointensities from the Mediterranean region that help to better constrain geomagnetic field intensity changes in Europe between 200 CE and 1600 CE. The new data have been obtained from the Thellier classical method including pTRM checks and both the TRM anisotropy and cooling rate corrections. The results, together with previous selected intensities, confirm the presence of five intensity maxima in Europe over this period. In particular, the new archeointensities are key to define the starting point of the double-oscillation feature that occurred in Europe during the second half of the first millennia CE, and reinforce the existence of a relative maxima around 1400-1450 CE in Western Europe. Finally, an analysis at continental scale of selected archeointensities covering the period 200 CE – 1600 CE suggests that the Western and Eastern European intensity maxima did not occurred simultaneously.

Key Words: Archeomagnetism, archeointensity, geomagnetic field strength maxima, paleomagnetism, Mediterranean.

1. Introduction

Nowadays, it is well known that the past geomagnetic field strength has exhibited numerous intense, short-lived (multidecadal) maxima at different times and locations (eg. Ertepinar et al., 2012; Hervé et al., 2013; Shaar et al., 2016). For the last two millennia several maxima have been also identified. In particular, the Western European region is characterized by a trend of intensity oscillation with five intensity maxima over the last 1500 years (Gómez-Paccard et al. 2012, 2016; Genevey et al., 2016, 2019). The occurrence of these intensity oscillations has also been suggested for Eastern Europe (Gómez-Paccard et al., 2012; Kovacheva et al., 2014, Genevey et al., 2016). Among these, the most important intensity feature identified is the double-oscillation that took place during the second half of the first millennium CE characterized by the highest intensities of the last 2 millennia. Whereas this double-oscillation is clearly identified in France (Gómez-Paccard et al., 2012, 2016; Genevey et al., 2016) and Bulgaria (Kovacheva et al., 2014), it is not well recovered in other European regions due to the low number of available archeointensities covering this period. This is the case of the Iberian Peninsula, Germany and Finland. In the Iberian Peninsula, the last paleosecular variation curve does not clearly show the double-oscillation although it is suggested by recent data (Molina-Cardín et al., 2018). In Germany (Schnepp et al., 2020) or Finland (Pesonen et al., 1995) high intensities have also been obtained for this period, but the double-oscillation is not well recovered by the few data available for this period. After this feature a succession of several minor intensity maxima have also been described in Europe, at the beginning of the 12th century CE, at the end of the 14th century CE and at the very beginning of the 17th century CE (Genevey et al., 2016). However, and despite the great effort made in the previously mentioned studies, the spatial and temporal extension of these maxima is not perfectly described all over Europe. For instance, it is

not clear if these events were simultaneously observed or not all over Europe (Gómez-Paccard et al., 2012; Genevey et al., 2016; Schnepp et al., 2020). In this context, here we present a complete paleomagnetic study of baked archeological materials collected in six archeological sites located in Spain, Greece and Italy (Fig. 1) with ages ranging between 400 CE and 1600 CE. These new data together with previous selected intensities allow us to give a further step in the description of past geomagnetic field intensity in Europe for the last two millennia.

2. Materials and methodology

The studied collection (Fig. 1) includes 54 ceramic fragments collected in 4 different archeological contexts (400-625 CE) located in the Balearic Islands (MC, ESC, CS and F sites), 6 tiles and 6 hand samples from a Greek kiln dated between 500 and 600 CE (VE site) and 12 samples from a 15^{th} century kiln from Italy (SAN site). At first glance, the studied potteries are red fine-grained fragments fairly homogeneous in their composition with no distinctive inclusions. The tiles and kiln´s samples, taken from the walls, were all red baked clays heated to high temperatures. In the Supporting Information a brief description of the archeological context and dating of the studied material together with the most relevant references is given.

Between 1 and 4 specimens per sample (106 in total) were prepared and studied. To determine archeointensities, we followed the Thellier classical method including partial thermoremanent magnetization (pTRM) checks and TRM anisotropy and cooling rate corrections. Rock-magnetic experiments were conducted to identify the main magnetic minerals carrying the thermoremanence of the samples. Most of the experiments were carried out at the paleomagnetic laboratory of the Complutense University of Madrid, but

some specific measurements were performed in the CIMaN-ALP Alpine paleomagnetic laboratory (Italy) and the paleomagnetic laboratory of the Aristotle University of Thessaloniki (Greece). The laboratory procedures followed are detailed in Rivero-Montero et al. (2021). Additionally, First Order Reversal Curve (FORC) experiments were carried out at the Institut de Physique du Globe de Paris (Paris) and the IGGL Geomagnetic Laboratory (Norway) with a magnetometer (μ-VSM) from Princeton Measurements Corporation. The FORC diagrams were measured with an averaging time of 100 ms with saturating field of 1.5 T and 250 FORCs by FORC diagram. To analyse the FORC diagrams, we used the VARIFORC software of Egli (2013).

Following our previous works, we applied several quality criteria at specimen level and only high-quality archeointensities determinations were retained. In addition, we calculated a mean value per archeological group by averaging the intensities obtained at the specimen level, defining an archeological group as the potteries of the same archeological level or the hand samples of a kiln or tile. Only the mean values derived from at least 3 specimens were retained. Additional details of the selection criteria can be found in Rivero-Montero et al. (2021).

3. Results

3.1. Rock magnetism

Initial NRM intensities vary between $2.0 \cdot 10^{-4}$ and $2.5 \cdot 10^{-2}$ Am^2/kg. Magnetic hysteresis cycles are closed with non-constricted loops that saturate at about 150–300 mT and with coercivities in the range of 4 and 16 mT (Fig. S1A and D) suggesting the dominance of low coercivity minerals. Isothermal remanent magnetization (IRM) acquisition experiments up to 500 T (Fig. S1B and E) show that the majority of the samples saturate

between 150–300 mT. However few samples do not completely saturate at the maximum applied field of 500 mT. Reversal of IRM acquisitions show a decrease of the remanence when switching the field, indicating a significant superparamagnetic (SP) fraction (Fig. S1E). IRMs up to 2T and further thermal demagnetization of IRM-cross components (Lowrie, 1992) confirm the presence of magnetite as the main carrier of magnetization. Some samples also show epsilon hematite phase (VE11, Fig S1I and G). The magnetic hysteresis-derived parameters were plotted on the Day-Dunlop plot (Dunlop, 2002). All the studied samples fall in single domain (SD) and pseudo-single domain (PSD) region of the Day-Dunlop plot (Fig. S1G). However, some samples deviate from the general behaviour and are shifted to the right or up, very likely due to the presence of SD and/or high coercivity minor traces. In the majority of the FORCs diagrams we can see the presence of two peaks: one very close to the origin with vertical contours characteristic of SP grains, and one centered at coercivities of around 4-16 mT, that might be attributed to stable SD grains (Roberts et al., 2000), see figures S1C and F. Curie temperatures between 530 and 580 ºC and the shape of K-T curves suggest the presence of magnetite/titanomagnetite with variable Ti content. In some K-T curves, the samples show a small increase in the susceptibility in the range of 300–350º C (Kontny and Grothaus, 2017), suggesting the presence of maghemite (Fig. S1H). The rock magnetic experiments (and Thellier experiments as will be explained in the next section) justify that the magnetic signal is dominated by SD or mainly SD particles.

3.2. New archeointensities

The 63.2% of the studied specimens show linear NRM-TRM diagrams with a single component of magnetization going towards the origin in the Zijderveld plots that is well isolated, after a small viscous component, between 100-200ºC and 440-560ºC (Fig. 2S

A). No evidence of multidomain grain behavior was observed in the selected samples since no curvature in the NRM/TRM plots was seen. The linearity of the selected experiments clearly indicates the dominance of SD magnetic grains in the selected samples. In other cases, complex behaviors are observed, with several components of magnetization, concave up behavior or evidences of important mineralogical changes during Thellier experiments (Fig. 2SB). Such specimens were rejected for paleointensity determination. Successful results are summarized in Table S1 of the Supplementary Material. As expected, the mean value of the TRM anisotropy effect is higher for the studied potteries and tiles (12.3%) than for the kilns (0.6%) with very similar values before and after this correction. The mean cooling rate (CR) effect value is 7.6%, with the highest values for the tiles (of about 15%). When the CR was not estimated due to evidence of alteration at high temperatures, we applied a mean value derived from the CR effect measured for the other specimens of the same group, or if this was not possible, we applied 5% decrease in paleointensity estimations (Genevey et al., 2008). The mean intensities are given in Table 1 and range between 51.7 and 68.0 μT corresponding to Virtual Axial Dipole Moment (VADM) values between 90 and 119 ZAm^2. The new data obtained from the Balearic Islands (Spain) support the presence of a rapid intensity increase, indicating a variability of about 16 μT (or 29 ZAm^2 in terms of VADM) between 400 to 625 CE (see Fig. 2A), corresponding to the initial phase of the double-oscillation. The results obtained from the tiles and wall's samples from the kiln sampled at Velika (Greece) are very consistent between them suggesting a 60-63 μT intensity for this location during the 6^{th} century CE. The new Greek data allow a better constrain of the geomagnetic strength field during the initial increase phase of the double-oscillation in Eastern Europe (Fig. 2B). Finally, a mean value of about 59 μT was obtained for Santhià

(Italy), giving additional information to define the relative maximum achieved at the beginning of the 15th century CE.

4. Discussion.

In order to refine the reconstruction of geomagnetic field strength changes in Europe between 200 CE and 1600 CE, we compiled the European archeointensities using the GEOMAGIA50v3.4 database just updated in January 2021 (Brown et al., 2015). From this compilation, we selected archeointensities obtained from 3 or more specimens and derived from Thellier type methods including partial pTRM checks. For potteries or highly anisotropic materials, only data considering the correction of the TRM anisotropy effect upon intensity estimates were selected. Following the results of Genevey et al. (2008), a 5 % decrease of the intensity values was applied when the CR correction factor was not experimentally determined. After this selection, we only retained data falling within an area of 7º of radius (~780km) centred in two locations: 45ºN / 5ºE for Western Europe and 45ºN / 25ºE for Eastern Europe (see dark blue and orange circles in Fig. 3). From 200 CE to 1600 CE, there were available 117 data from Western Europe, and 72 from Eastern Europe.

From the compiled datasets and the new data presented here, we obtained two new intensity paleosecular variation (PSV) curves for Western and Eastern Europe (Fig. 2). The PSV curves were fitted using temporal cubic b-splines in a bootstrap approach that takes into account both age and intensity uncertainties (see Rivero-Montero et al., 2021 for more details). The two curves clearly show five intensity maxima between 200 and 1600 CE. However, it seems that the maxima were achieved at different times in Western and Eastern Europe and reached different intensity maximum values. According to the

PSV curves, for Western Europe (Fig. 2A) the maxima occurred around 310 CE, 620 CE and 820 CE (corresponding to the double-oscillation), 1140 CE and 1380 CE; with maximum values of 62.8 μT, 76.6 μT, 77.0 μT, 59.3μT and 55.5 μT, respectively. Whereas in Eastern Europe (Fig 2B), the five maxima are identified at 350 CE, 670 CE, 940 CE, 1300 CE and 1580 CE, with intensities of 59.0 μT, 72.4 μT, 74.4 μT, 56.8 μT and 61.0 μT, respectively. In this case, the highest intensities of the double-oscillation were achieved at 670 CE and 940 CE. Therefore, the five maxima are observed some decades later in the Eastern side of Europe. This time elapse between maxima is further analyzed below.

Additionally, the new PSV curves are compared with previous PSV curves and with the predictions derived from different global archeomagnetic models (see Figs. 2C and D). In Western Europe (Fig. 2C), the previous PSV curve of Gómez-Paccard et al. (2016) did not clearly exhibited the small maximum identified now at 310 CE. The double-oscillation feature (620 CE and 820 CE) was already recorded in previous curves but showing a smoother behaviour (Genevey et al., 2016) or lower intensity values (Gómez-Paccard et al., 2016) than those provided by our new PSV curve. Finally, a good agreement is found between previous curves and models for the last two maxima (1140 CE and 1380 CE). The global models show a clear smoother behaviour during the whole period, although the SHAWQ2k model seems to fit better the double-oscillation feature. This could be probably related with the fact that this global reconstruction involved more recent data than the ARCH10k.1 model and/or to the data-weighting scheme used in the SHAWQ2k (see Campuzano et al., 2019).

In Eastern Europe (Fig. 2D), the previous PSV curves show different behaviours. The Bulgarian curve (Kovacheva et al., 2014) shows a trend of oscillations, including the double-oscillation feature, with significant amplitudes (corresponding to rates of change up to 21.5 μT/century). Since neither our selected high-quality dataset nor the new PSV curve present this high variability, we suggest that some of the Bulgarian maxima and minima are controlled by some archeointensities that do not accomplished modern standards of quality. Although the Gómez-Paccard et al. (2016) curve also exhibits the double-oscillation feature around 670 and 940 CE, this curve seems very smoothed for the other periods. It is important to note that the double-oscillation shows a stronger decline in intensity between the two peaks in Eastern (with a minimum of 56.2 μT) than in Western Europe (with a relative minimum of 68.4 μT). This difference might be related to the low number of data (4) available for Eastern Europe for describing the minimum (Kovacheva et al., 2014 and Spatharas et al., 2011). Global models show smoother trends for the intensity element at these regional scales and are not able to completely reproduce the double-oscillation.

Since the double-oscillation is the most important feature of the European geomagnetic field strength over the last 2 millennia, we also evaluated the time and spatial evolution of this event throughout this continent. To do that, we obtained the PSV curves for 5 additional regions (7º of radius) in Europe following the same methodology used before (see map in Fig 3A). Despite the great effort made during the last years, the number of archeointensities is still very low for some of the selected regions. For example, in Iberia the lack of data between 600 and 800 CE has not allowed to identify the minimum between the two maxima of the double-oscillation and, hence, a single maximum is seen in the PSV curve. In central Europe, the PSV curves of the regions “50ºN / 15ºE” and

242 "47.5ºN / 20ºE" are not well defined between 500 and 700 CE and 700 and 850 CE,
243 respectively, due to the low number of data available. Despite these gaps, a general view
244 of geomagnetic field changes in Europe can be deduced. Results from Fig. 3 suggest a
245 decrease of the VADM from Western to Eastern Europe. For example, the VADM of the
246 double-oscillation in Western Europe achieved values around 125 ZAm^2 (dashed lines in
247 figure 3A) whereas in Eastern Europe the VADMs are lower (around 120 ZAm^2,
248 continuous lines in figure 3A). Furthermore, as indicated below, there is a time delay
249 between the five maxima observed, being those from Western Europe recorded several
250 decades before. According to Fig. 3b, the time delay between the maxima increases from
251 ancient to modern times: 40, 50, 120, 160 and 200 yr for the first, second, third, fourth
252 and fifth maxima, respectively. This could indicate an eastward drift of a regional
253 intensity patch at the core-mantle boundary beneath Europe that is progressively
254 attenuated with time generating the succession of these maxima observed at the surface.
255 Our study also suggests that the period of recurrence of the maxima, estimated in about
256 290 ± 50 yr, is similar in Western Europe and Eastern Europe. This result is in agreement
257 with the period of 250 years proposed by Genevey et al. (2016) for Western Europe and
258 interpreted as a particular characteristic of the secular variation in the region probably
259 related to a wave motion in the liquid core (e.g. Finlay and Jackson, 2003; Buffett, 2014).
260
261
262 **Acknowledgments**
263 This research has been funded by the CGL2015-63888-R and PGC2018-099103-A-I00
264 projects and the FPI BES-2016-077257 grant of the Ministerio de Ciencia, Innovación y
265 Universidades (Spain). We extend our warm thanks to our colleagues of the IPGP (Paris),

266 especially to France Lagroix and Jean-Pierre Valet, where the FORCS measurements
267 were performed.
268
269
270 **Figure captions**
271

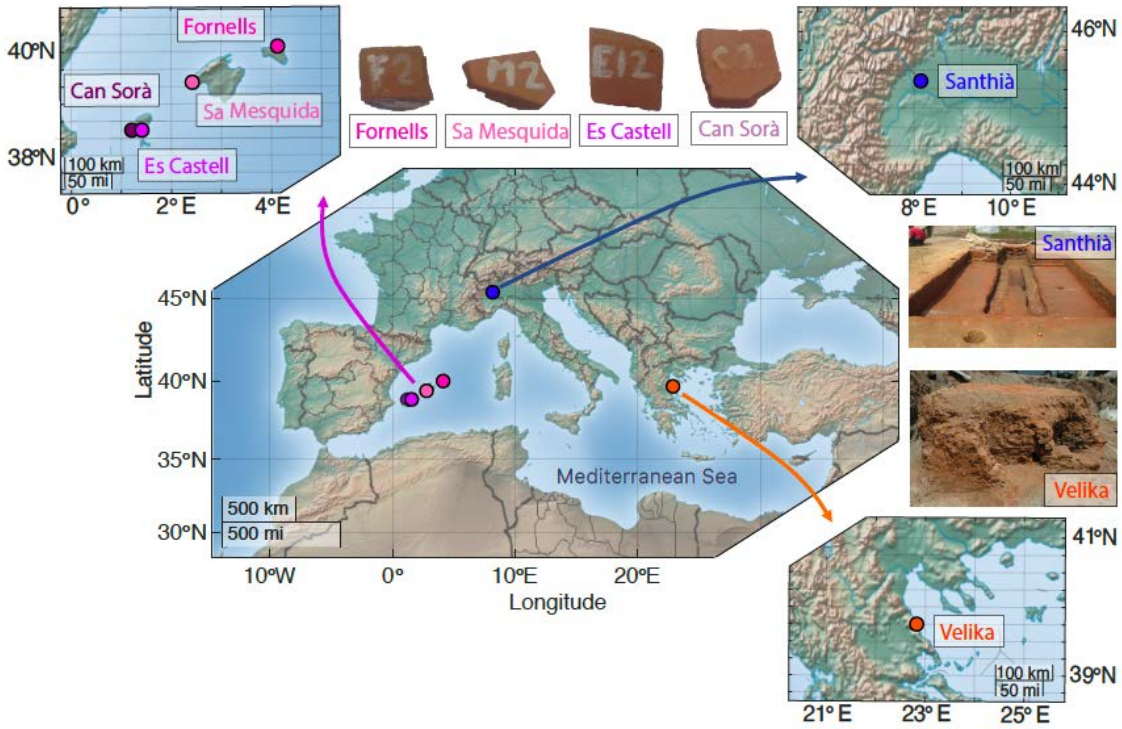

272
273 **Figure 1**. Location of the studied archeological sites where the archeological materials
274 were recovered and pictures of representative potteries and kilns.
275

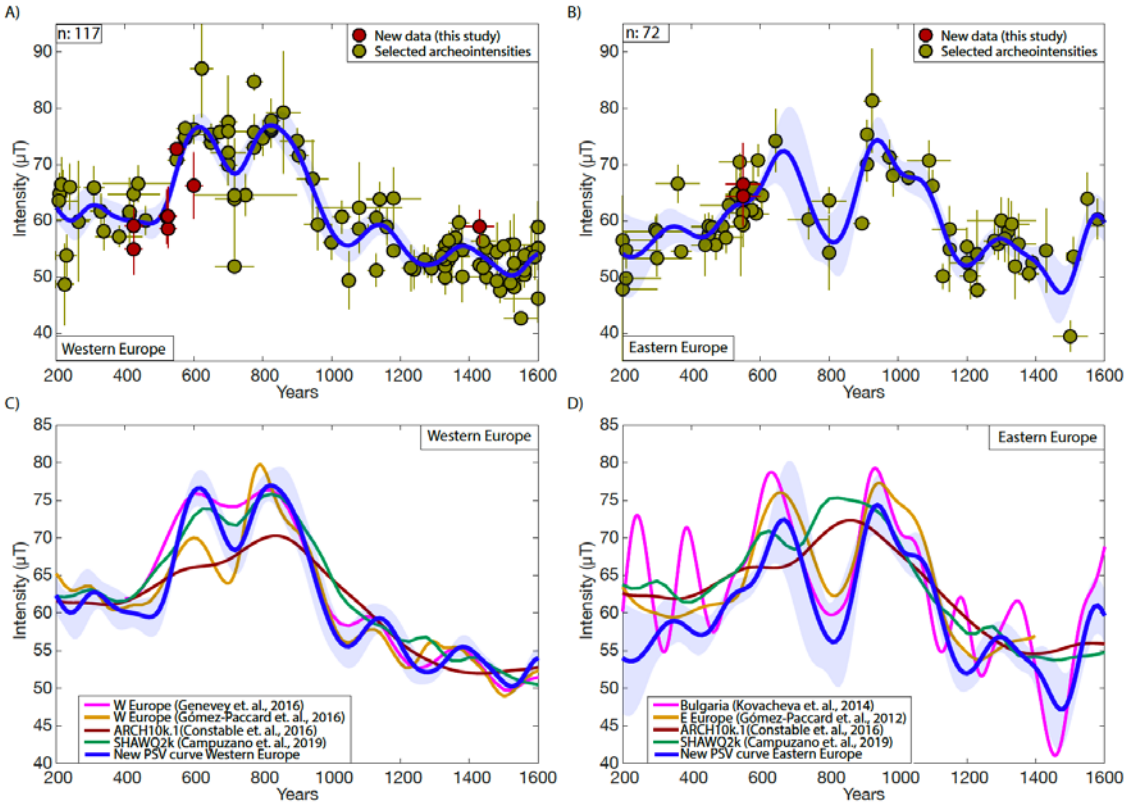

Figure 2. New archeointensity results (red circles) obtained from at least 3 specimens and following the selection criteria explained in Rivero-Montero et al. (2021) together with previous selected results (green circles). **n**: is the number of data represented at each figure. The new PSV curves (blue lines) together with its 1-sigma error band (shaded areas) are also showed. Previous PSV regional curves and different global models results are also represented. Data, curves and models are all relocated to 45º N, 5º E for Western Europe and 45º N, 25º E for Eastern Europe.

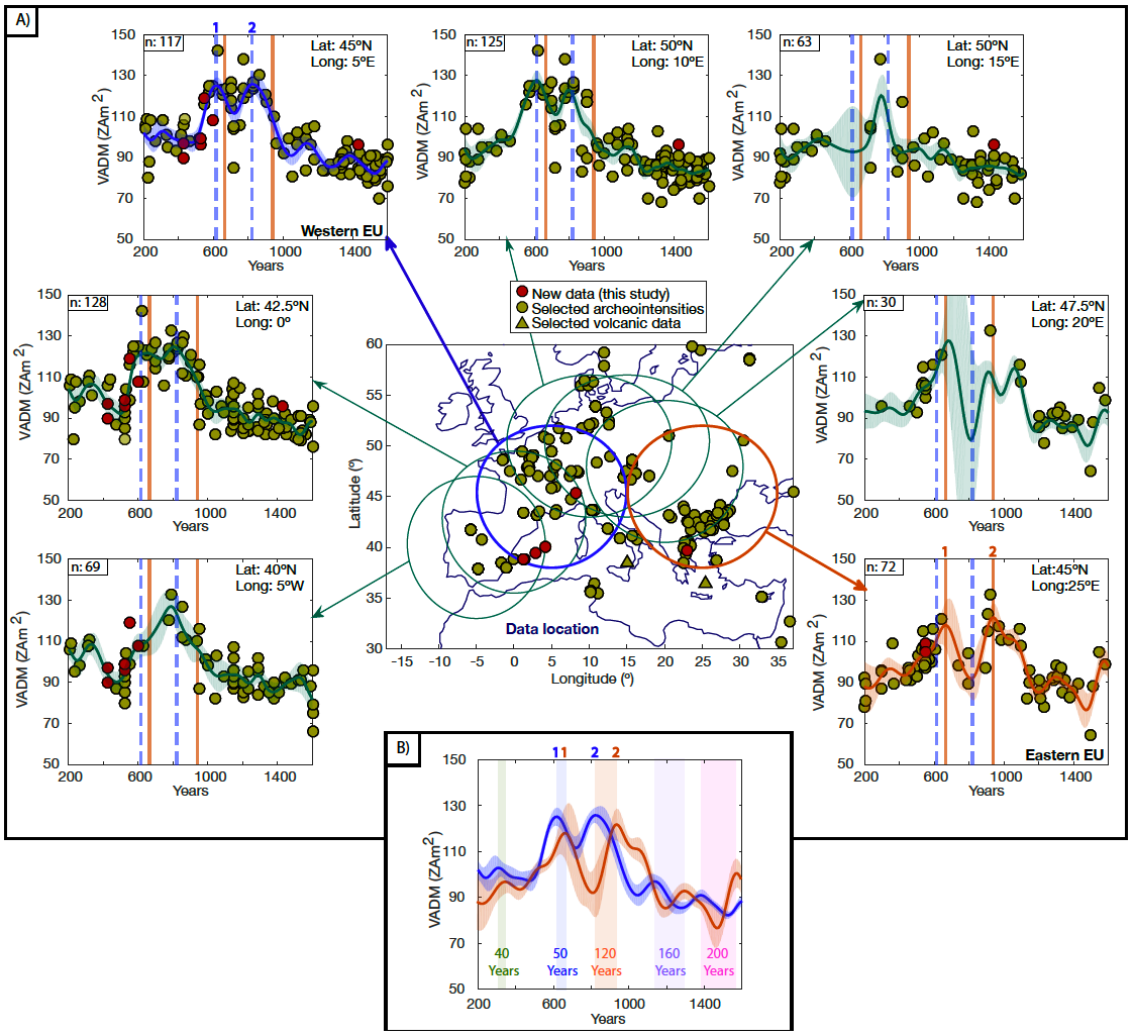

285

286 **Figure 3**. A) PSV intensity curves between 200 CE and 1600 CE calculated for different
287 regions, being the regions represented by circles in the central map. **n**: is the number of
288 data represented at each figure. The shaded areas represent the 1-sigma error band of the
289 curves. The new data obtained here are shown in red circles and previous data from other
290 studies in green. The dashed lines corresponding to the maxima in Western Europe (620
291 CE and 820 CE) and the continuous lines corresponding to the maxima in Eastern Europe
292 (660 940 CE). B) PSV intensity curves, in blue Western Europe and in orange Easter
293 Europe. The shaded areas show the temporary differences between the five maxima of
294 Western and Eastern Europe.

295

296

297 **Table captions**

298 **Table 1**.

299 Summary of the new archeointensities obtained for the Western and Eastern Europe.
300 Country: country of origin; Site: name of the archeological site; Lat. and Long.:
301 geographical coordinates. Material and Lab code: Material and Laboratory code for the
302 studied collection; Date: indicates the age ascribed to each group; N (n): number of
303 samples (specimens) retained to calculate mean intensities; F ± sd: mean intensity and
304 standard deviation before corrections; F_{ATRM} ± sd: mean intensity and standard deviation
305 corrected for the TRM anisotropy effect; F_m ± sd: mean intensity and standard deviation
306 corrected for the TRM anisotropy and cooling rate effects upon archeointensity estimates;
307 σb/Fm: standard error/mean intensity; VADM: values of the virtual axial dipole moment.

308

309 **References**

310 Brown, M.C., Donadini, F., Korte, M., Nilsson, A., Korhonen, K., Lodge, A., Lengyel,
311 S.N., Constable, C.G., 2015. GEOMAGIA50.v3: 1. General structure and modifi-
312 cations to the archeological and volcanic database. Earth Planets Space, 67, 83.
313 https://doi .org /10 .1186 /s40623 -015 -0232 -0.

314 Buffett, B., 2014. Geomagnetic fluctuations reveal stable stratification at the top of
315 the Earth's core. Nature 507, 484–486. http://dx.doi.org/10.1038/nature13122.

316 Campuzano, S.A., Gómez-Paccard, M., Pavón-Carrasco, F.J., Osete, M.L., 2019.
317 Emergence and evolution of the South Atlantic Anomaly revealed by the new
318 paleomagnetic reconstruction SHWQ2k. Earth Planet. Sci. Lett., 512, 17-26.

319 Constable, C., Korte, M., Panovska, S., 2016. Persistent high paleosecular variation
320 activity in southern hemisphere for at least 10 000 years. Earth and Planetary Science
321 Letters, 453, 78-86.

322 Dunlop, D.J., 2002. Theory and application of the Day plot (Mrs/Ms versus Hcr/Hc) 1.
323 Theoretical curves and tests using titanomagnetite data. J. Geophys. Res., Solid Earth,
324 107(B3), EPM-4.
325 Egli, R., 2013. VARIFORC: An optimized protocol for calculating non-regular first-order
326 reversal curve (FORC) diagrams. Global and Planetary Change, 110, 302-320.
327 Ertepinar, P., Langereis, C.G., Biggin, A.J., Frangipane, M., Matney, T., Okse, T., Engin,
328 A., 2012. Archaeomagnetic study of five mounds from Upper Mesopotamia between
329 2500 and 700 BC: further evidence for an extremely strong geomagnetic field ca. 3000
330 years ago. Earth Planet. Sci. Lett., 357, 84-98.
331 Finlay, C.C., Jackson, A., 2003. Equatorially dominated magnetic field change at the
332 surface of the Eath's core. Science 300, 2084–2086.
333 Genevey, A., Gallet, Y., Constable, C. G., Korte, M., Hulot, G., 2008. ArcheoInt: An
334 upgraded compilation of geomagnetic field intensity data for the past ten millennia and
335 its application to the recovery of the past dipole moment. Geochem. Geophys.
336 Geosyst., 9(4), Q0438.
337 Genevey, A., Gallet, Y., Jesset, S., Thébault, E., Bouillon, J., Lefèvre, A., Le Goff, M.,
338 2016. New archeointensity data from French Early Medieval pottery production (6th–
339 10th century AD). Tracing 1500 years of geomagnetic field intensity variations in
340 Western Europe. Physics of the Earth and Planetary Interiors, 257, 205-219.
341 Genevey, A., Principe, C., Gallet, Y., Clemente, G., Le Goff, M., Fournier, A., Pallecchi,
342 P., 2019. Refining the high-fidelity archaeointensity curve for Western Europe over
343 the past millennium: Analysis of Tuscan architectural bricks (Italy). Geological
344 Society., London, Special Publications.
345 Gómez-Paccard, M., Chauvin, A., Lanos, P., Dufresne, P., Kovacheva, M., Hill, M. J.,
346 Beamud, E., Blain, S., Bouvier, A., Guibert, P., Archaeological Working Team, 2012.

Improving our knowledge of rapid geomagnetic field intensity changes observed in Europe between 200 and 1400 AD. Earth Planet. Sci. Lett., 355–356, 131–143.

Gómez-Paccard, M., Osete, M.L., Chauvin, A., Pavón-Carrasco, F.J., Pérez-Asensio, M., Jiménez, P., Lanos, P., 2016. New constraints on the most significant paleointensity change in Western Europe over the last two millennia. A non-dipolar origin? Earth Planet. Sci. Lett., 454, 55-64.

Hervé, G., Chauvin, A., Lanos, P., 2013. Geomagnetic field variations in Western Europe from 1500 BCE to 200 AD. Part II: New intensity secular variation curve. Phys. Earth Planet. Inter., 218, 51-65.

Kontny, A., Grothaus, L., 2017. Effects of shock pressure and temperature on titanomagnetite from ICDP cores and target rocks of the El'gygytgyn impact structure, Russia Stud. Geophys. Geod., 61, 163-183.

Kovacheva, M., Kostadinova-Avramova, M., Jordanova, N., Lanos, P., Boyadzhiev, Y., 2014. Extended and revised archaeomagnetic database and secular variation curves from Bulgaria for the last eight millennia. Phys. Earth Planet. Inter., 236, 79-94.

Lowrie, W. ,1990. Identification of ferromagnetic minerals in a rock by coercivity and unblocking temperature properties. Geophys. Res. Lett., 17, 159–162. https://doi.org/10.1029/GL017i002p00159.

Molina-Cardín, A., Campuzano, S.A., Osete, M.L., Rivero-Montero, M., Pavón-Carrasco, F.J., Palencia-Ortas, A., Martín-Hernández, F., Gómez-Paccard, M., Chauvin, A., Guerrero-Suárez, S., Pérez-Fuentes, J.C., McIntosh, G., Catanzariti, G., Sastre-Blanco, J.C., Larrazabal, J., Fernández-Martínez, V.M., Álvarez-Sanchís, J.R., Rodríguez-Hernández, J., Martín-Viso, I., García I Rubert, D., 2018. Updated Iberian archeomagnetic catalogue: new full vector paleosecular variation curve for the last

three millennia. Geochem. Geophys. Geosyst., 19, 3637-3656. https://doi.org/10.1029/2018GC007781.

Rivero-Montero, M., Gómez-Paccard, M., Kondopoulou, D., Tema, E., Pavón-Carrasco, F. J., Aidona, E., Campuzano, SA, Molina-Cardín A, Osete ML, Palencia-Ortas A, Martin-Hernándes F, Rubat-Borel F, Venturino, M. Geomagnetic field intensity changes in the Central Mediterranean between 1500 BCE and 150 CE: Implications for the Levantine Iron Age Anomaly evolution. Earth and Planetary Science Letters, 557, 116732.

Roberts, A. P., Pike, C. R., Verosub, K. L., 2000. First-order reversal curve diagrams: A new tool for characterizing the magnetic properties of natural samples. Journal of Geophysical Research: Solid Earth, 105(B12), 28461-28475.

Schnepp, E., Thallner, D., Arneitz, P., Leonhardt, R., 2020. New archeomagnetic secular variation data from Central Europe, II: Intensities. Physics of the Earth and Planetary Interiors, 309, 106605.

Shaar, R., Tauxe, L., Ron, H., Ebert, Y., Zuckerman, S., Finkelstein, I., Agnon, A. 2016. Large geomagnetic field anomalies revealed in Bronze to Iron Age archeomagnetic data from Tel Megiddo and Tel Hazor, Israel. Earth Planet. Sci. Lett., 442, 173-185.

Spatharas, V., Kondopoulou, D., Aidona, E., Efthimiadis, K. G. (2011). New magnetic mineralogy and archaeointensity results from Greek kilns and baked clays. Studia Geophysica et Geodaetica, 55(1), 131-157.

Tema, E., Lanos, P., 2020. Full vector calibration curve for Italy based on a revised compilation of archaeomagnetic data: Insights on secular variation and implications on dating. Archaeometry.